JACS
JOURNAL OF THE AMERICAN CHEMICAL SOCIETY

Article

pubs.acs.org/JACS

Self-Assembled Pyridine-Dipyrrolate Cages

Huacheng Zhang,[†] Juhoon Lee,[†] Aaron D. Lammer,[†] Xiaodong Chi,[†] James T. Brewster,[†] Vincent M. Lynch,[†] Hao Li,[‡] Zhan Zhang,[†,§] and Jonathan L. Sessler*[,†,§]

[†]Department of Chemistry, The University of Texas at Austin, Austin, Texas 78712-1224, United States

[‡]Department of Chemistry, Zhejiang University, Hangzhou 310027, China

[§]Institute for Supramolecular and Catalytic Chemistry, Shanghai University, Shanghai 200444 China

Supporting Information

ABSTRACT: An inherently nonlinear pyridine dipyrrolate ligand, namely 2,6-bis(3,4-diethyl-5-carboxy-1*H*-pyrrol-2yl)pyridine (compound **1**), is able to distinguish between different zinc(II) cation sources, namely $Zn(acac)_2$ and $Zn(OAc)_2$, respectively. This differentiation is manifest both in terms of the observed fluorescent behavior in mixed organic media and the reaction chemistry. Treatment of **1** with $Zn(acac)_2$ gives rise to a cage dimer, cage-**1**, wherein two molecules of compound **1** act as double bridging units to connect two individual cage subunits. As inferred from X-ray crystallographic studies, this cage system consists of discrete zinc dimers with hydroxide bridges that, with the assistance of bound DMF solvent molecules, serve to fix the geometry and orientation of the pyridine dipyrrolate building blocks. When a different zinc source, $Zn(OAc)_2$, is used to carry out an ostensibly similar complexation reaction with compound **1**, an acetate-bridged 1D abacus-like cage polymer is obtained as inferred from X-ray diffraction analysis. This extended solid state structure, cage-**2**, contains individual zinc dimer cage submits and appears stabilized by solvent molecules (DMF) and the counteranion (acetate). Rod-like assemblies are also observed by DLS and SEM. This construct, in contrast to cage-**1**, proved fluorescent in mixed organic media. The structure of the ligand itself (i.e., in the absence of Zn(II)) was confirmed by X-ray crystallographic analysis and was found to assemble into a supramolecular polymer. Conversion to a dimer form was seen upon the addition of TBAOAc. On the basis of the metric parameters, the structures seen in the solid state are stabilized via hydrogen bonding interactions involving solvent molecules.

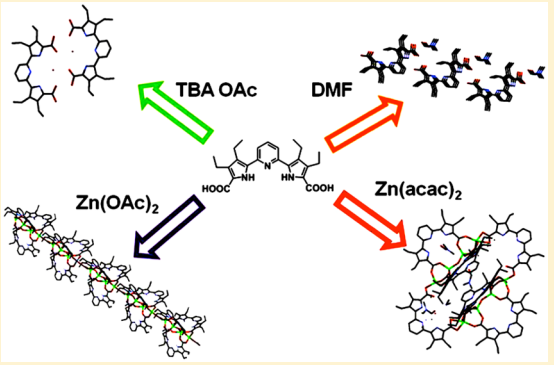

INTRODUCTION

The synthesis of rationally designed materials with small, well-defined lacuna represents one of the most vibrant topics in inorganic and organic chemistry. Such cage systems are finding application in a number of areas, including supramolecular chemistry,[1] catalysis,[2] coordination polymers and MOFs,[3] nanomaterials,[4] and crystal-free crystallography.[5] Both metal-free[1] and metal cation-driven approaches[3] have been explored extensively in recent years to create through self-assembly systems with novel shapes, sizes, and internal void dimensions.[1] Among the current challenges is understanding how the molecular features of the constituent precursors, or molecular building blocks, become translated into specific assemblies under the conditions of self-assembly.[3b,5] New insights into the fundamental determinants, as well as potentially novel self-assembled materials,[1] can come from explorations of molecular-scale components that assemble into different structures in the presence and absence of ostensibly similar self-assembly inducing inputs, such as coordinating metal cations.[3b] Here, we report a new bis-anionic ligand, an inherently "bent" pyridine dipyrrolate, that assembles to create two very different cage-containing assemblies, discrete multicyclic and abacus-like polymeric, respectively, upon exposure to two different zinc cation precursors. This system also self-associates to produce infinitely repeating zigzag-shaped supramolecular polymers in the absence of a Zn(II) source. These self-assembled materials can be modified through changes in the external environment, such as variations in the effective pH or choice of ancillary ligand, with attendant changes in the physical and optical properties being observed. The present system acts as a unique chemosensor in that it is able to differentiate between two common zinc(II) cation forms, as well as more common response-inducing triggers, such as protonation state and solvent. The present constructs also serve to highlight how very different extended structures may be obtained from ostensibly similar starting materials. This work is thus expected to increase our understanding of self-assembly and how the choice of precursors may be used to extend its range and utility.

Metal-directed self-assembly[6] is one of the most versatile and efficient methods to create coordination polymers, MOFs (metal−organic frameworks), and cages, in part because this

Received: January 22, 2016
Published: March 13, 2016

DOI: 10.1021/jacs.6b00564
J. Am. Chem. Soc. 2016, 138, 4573−4579

Scheme 1. Structural Formulas of Pyridine-Dipyrrolate 1, Cage-1, and Polymeric Cage-2

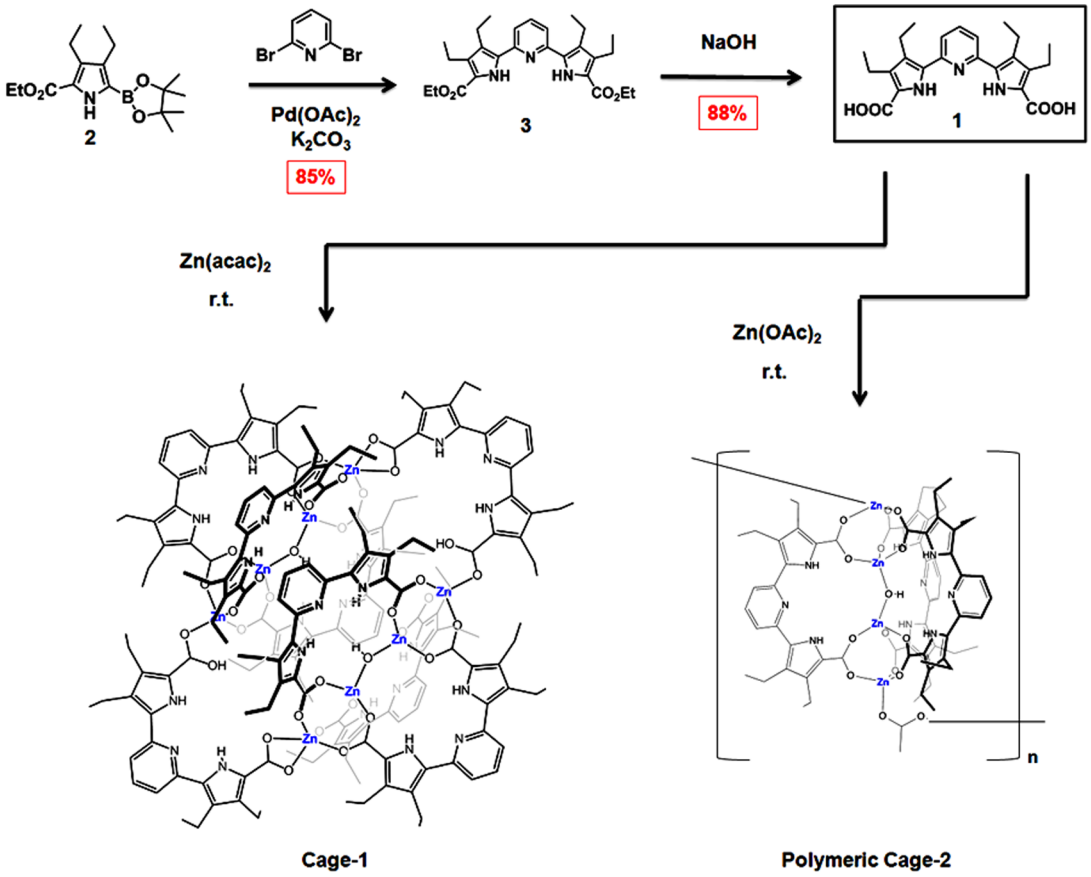

kind of self-assembly can afford elaborate, well-defined structures by using only simple organic ligands.[7] Because of its heavily studied complexation chemistry[8] and photophysically benign properties,[9] zinc(II) has played a central role in these efforts.[10,11] In the case of cages, zinc complexation studies have focused primarily on *N*-donors[12] or classic macrocycles,[13] e.g., macrocyclic polyamines,[14] porphyrins,[15] calixarenes,[16] cucurbiturils,[17] and pyrogalloarenes,[18] although macromolecules, e.g., proteins,[19] have been exploited as ligands.

Relatively little work has focused on the use of angular compounds as precursors. The pyridine dipyrrolate, 2,6-bis(3,4-diethyl-5-carboxyl-1*H*-pyrrol-2yl)pyridine (compound **1**, Scheme 1), provides two potential carboxylate donors at a very acute angle,[5] which stands in contrast to the linear dicarboxylate ligands typically used to prepare MOFs[20] and other self-assembled metal-directed self-assembled constructs.[5]

The pyridine dipyrrolate of the present study is an 18-π electron system that bears structural analogy to terpyridine.[21] In contrast to terpyridine, compound **1** and its analogues have not been extensively explored as ligands. The Setsune group[22] and our group[23] have used pyridine dipyrrolate as a building block to synthesize cryptand-like porphyrinoids and expanded porphyrins, respectively. A system analogous to **1**, but lacking the carboxylic acid functionality, namely 2,6-bis(2′-indolyl)-pyridine,[24] was found to act as a ligand for several transition metal cations, including palladium and platinum, as well as main-group metal cations including tin and lead. Very recently, Caulton et al.[25] reported a novel pyridine dipyrrolate-based pincer ligand, and studied its steric and electronic characteristics. However, neither the inherent self-assembly features nor the use of pyridine dipyrrolates to stabilize metal-directed coordination polymers or cages, have been reported as yet. As noted above and discussed in detail below, compound **1** not only undergoes self-assembly in the absence of a metal, it can stabilize two very different cage-containing structures when treated with differing zinc(II) sources, namely zinc acetylacetonate hydrate ($Zn(acac)_2$) and zinc acetate ($Zn(OAc)_2$). To our knowledge, the resulting structures are without precedent in the literature, as is the ability to distinguish between two ostensibly similar zinc(II) salt forms.

RESULTS AND DISCUSSION

Synthesis and Self-Assembly of 1 in the Presence of DMF. The synthesis of compound **1** is shown in Scheme 1. It involves two steps. Its ester form (compound **3**) was prepared in 85% yield through a palladium(II) acetate-catalyzed Suzuki–Miyaura cross-coupling reaction[26] using 2,6-dibromopyridine and a pyrrole boronic ester (compound **2**)[27] in a molar ratio of 1:2.4 as starting materials. Under these conditions, compounds **4** and **5**[28] (Scheme S1) are also obtained in low yield. Compounds **3**–**5** were characterized by NMR spectroscopy and mass spectrometry (see Supporting Information), with the data for **3** and **5** being in accord with the literature.[23]

After isolation, sodium hydroxide-mediated hydrolysis of compound **3** afforded compound **1** as a white powder in 88% yield. Compound **1** was characterized by NMR spectroscopy and mass spectrometry (see SI). Single crystals suitable for X-ray diffraction analysis, were grown through vapor diffusion of hexanes into an *N*,*N*-dimethylformamide (DMF) solution of **1**. The resulting structure, shown in Figure 1a and 1b, revealed

DOI: 10.1021/jacs.6b00564
J. Am. Chem. Soc. 2016, 138, 4573–4579

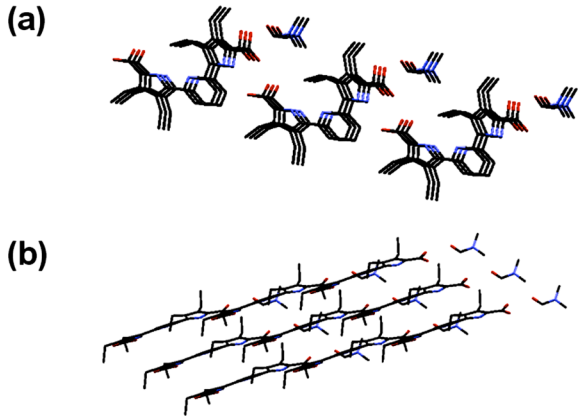

Figure 1. Crystal structures of compound **1**. Parts (a) and (b) show top view and side view with the stick framework of compound **1**. Color: C gray, N blue, O red. The hydrogen atoms are omitted for clarity.

that compound **1** adopts a conformation wherein the N−H moiety on one pyrrole are directed inward (NCCN dihedral angle 4.54°), to form an intramolecular hydrogen bond with the N on a neighboring pyridine. However, the N−H group on the other pyrrole is directed outward (NCCN dihedral angle 160.8°). The O−H of the carboxyl functionality in compound **1** forms an intermolecular hydrogen bond with the oxygen of a solvent molecule DMF (O−O = 2.578 Å). This interaction serves to fix the orientation of this pyrrole ring such that its N−H and C═O further hydrogen bond, respectively, to the C═O and H−O of a carboxylic acid (N−O = 3.013 Å, O−O = 2.595 Å) group on a pyrrole ring from a neighboring molecule of **1**. As a result, compound **1** exists in the form of an hydrogen bonded supramolecular polymer in the solid state. The individual supramolecular polymers are stacked upon one another with the shortest distance between each layer being 3.394 Å.

Variable temperature (VT) NMR spectroscopic analysis were carried out in DMF-d_7 to gain further insights into the presumed intermolecular hydrogen bonds that are proposed to stabilize the self-assembled constructs formed from **1**. Clear upfield shifts are seen for the *H*-pyrrole and *H*-carboxylate acid resonances upon passing from low to high temperature (cf. Figure S1). On this basis, we suggest that hydrogen bonds persist both at −50 °C and at room temperature, but are essentially absent at 100 °C. To the extent this inference is correct, it leads to the conclusion that the supramolecular polymer formed via the hydrogen bond-mediated self-assembly **1** is thermally responsive and can be disassembled by raising the temperature.

Dimer of 1 Produced upon Treatment with TBAOAC. The self-assembled ensemble produced from **1** proved environmentally responsive. Specifically, the addition of basic reagents, such as tetrabutylammonium acetate (TBAOAc), leads to discernible changes in the spectroscopic features of the system. For instance, a decrease in the fluorescent intensity (Figure S2) and an upfield shift in the pyridine proton resonances was observed in the emission and ^{1}H NMR spectra (Figure S3), respectively, upon the addition of one equivalent of TBAOAc. Such changes are consistent structural rearrangements that affect the local environment of the pyridine subunits. X-ray crystallographic analysis provided support for this latter inference (Figure S4). In particular, conversion to a dimeric form is observed (Scheme 2). Presumably, these structural changes are the direct result of TBAOAc-induced

Scheme 2. Crystal Structures and Reaction Chemistry Highlighting How Addition of TBAOAc to the Self-Assembled Polymer Produced from 1 in the Absence of Zinc(II) Gives Rise to a Discrete Dimer

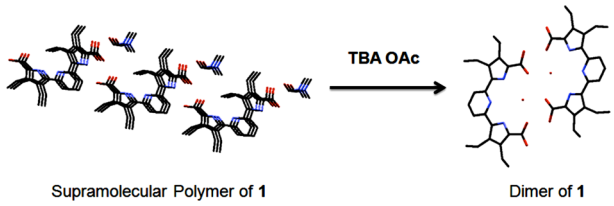

monodeprotonation and involve hydrogen bonding interactions between carboxylate groups on two different molecules of **1** (Figure S4). In contrast to what is seen for the diacid form of **1**, in the dimer the two pyrroles are directed inward, leading to new NCCN dihedral angles of 8.23 and 8.29°, respectively (Figure S5). An H_2O molecule is observed in the solid state that is hydrogen bonded to the N−H protons of the pyrroles (Figure S5). Such ancillary interactions likely serve to fix further the geometry of the monodeprotonated form of **1** within the dimer.

Formation of Cage-1 in the Presence of Zn(acac)$_2$. The importance of effective pH and the apparent role of residual solvent in stabilizing the solid state structures observed in the case of **1** led us to consider that the reaction conditions and external environment might likewise play a modulating role under conditions of zinc(II)-mediated self-assembly. As a first test of whether the angular nature of **1** would permit formation of a well-defined, metal cation-containing structure, one equivalent of Zn(acac)$_2$ was added into a solution of **1** in DMF-MeOH. Upon this addition, the sample solution undergoes obvious changes in both its color and fluorescent emission features (Figures 2, S6, and S7). Both a shift in the absorbance (so-called R band, from 270 to 300 nm) and decreased UV absorption intensity are observed in the UV−vis spectrum. A red-shift in the emission peak (Figure 2) and an enhancement in the intensity are observed in the fluorescence spectrum of **1** after treatment with one equiv of Zn(acac)$_2$.[29]

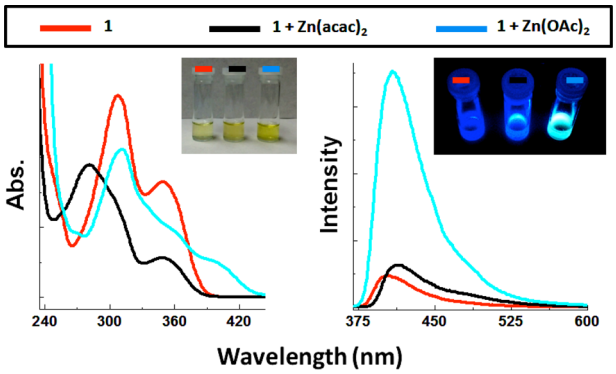

Figure 2. Changes of UV−vis ([**1**] = 10^{-5} M, left) and fluorescent emission spectra ([**1**] = 10^{-6} M, excited at 365 nm, right) from the sample solution of 1 (red line) seen upon the addition of **1** equivalent of either Zn(acac)$_2$ (black line) or Zn(OAc)$_2$ (blue line) in DMF-MeOH (1/5, v/v). Inset: Photographs of the sample solutions in question under visible light (left) and excited at 365 nm (right).

DOI: 10.1021/jacs.6b00564
J. Am. Chem. Soc. 2016, 138, 4573−4579

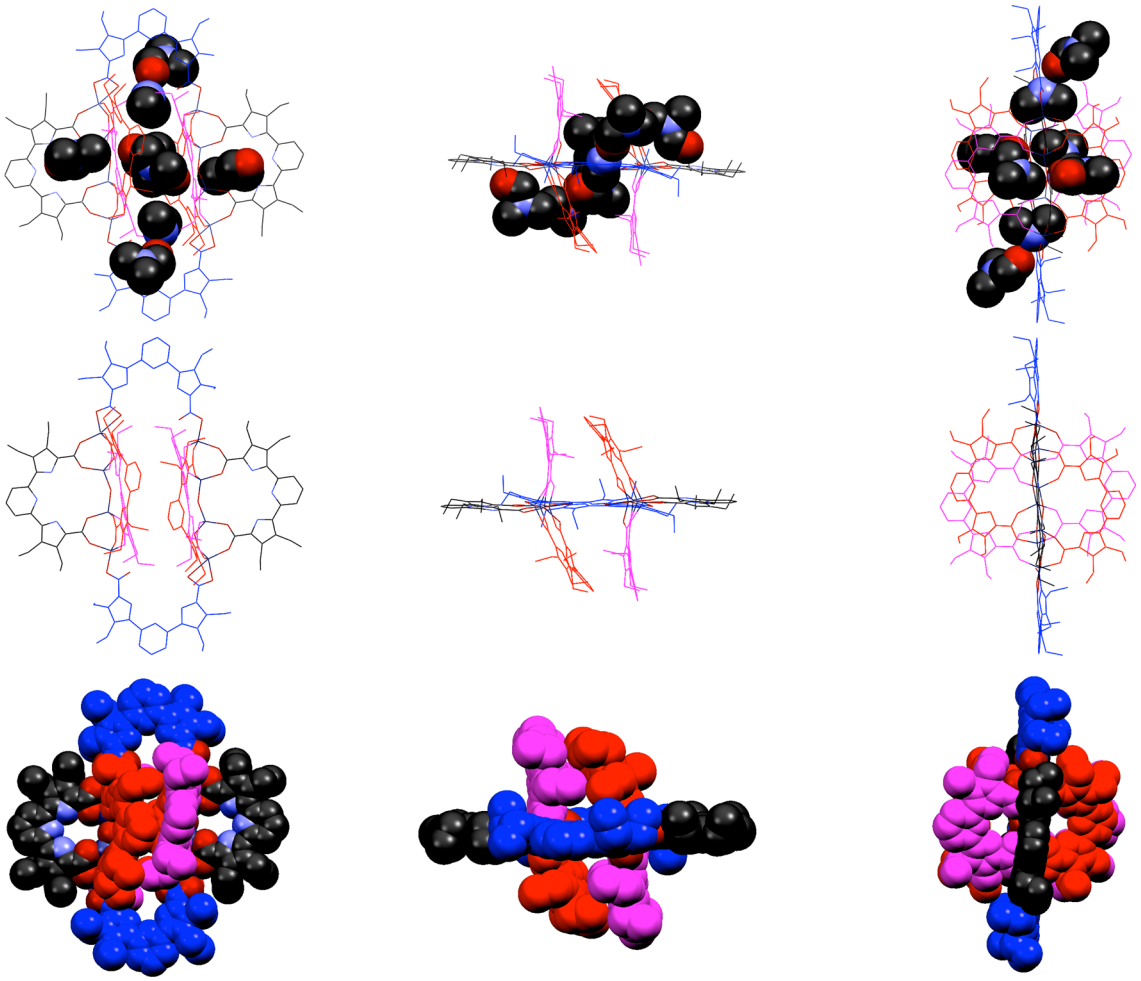

Figure 3. Coordination geometries of the Zn sites and ligand environments as deduced from the single crystal structures of cage-**1** viewed from the front (left), top (center), and side (right) in both wireframe (top and middle) and space-filling representations (bottom). The different subunits of **1** that make up the structure are shown in blue, red, magenta, and CPK coding, respectively. Solvent molecules are shown in the top view in space-filling form but omitted for clarity in the other views. The hydrogen atoms are omitted for clarity.

These findings are taken as initial evidence of Zn(II) complexation. A Job's plot derived from a fluorescent emission spectral titration, showed a maximum at a mole fraction of 0.5, as would be expected for the formation of a 1:1 complex (Figure S8). Upon the addition of this Zn(II) cation source, the pyridine proton signals of **1** undergo splitting and produced distinct chemical shifts in the ^{1}H NMR spectrum (Figure S9).

Colorless single crystals of the solid materials were obtained using a vapor diffusion procedure analogous to that described above. The resulting structure revealed that a cage-like Zn(II)-directed supramolecular ensemble is stabilized in the solid state as shown in Figure 3. The large cage structure sits around a crystallographic inversion center, and has eight molecules of compound **1** complexed to eight zinc(II) ions (Figure 3), in an overall 1:1 stoichiometric ratio, as inferred from the solution phase Job's plot analysis (Figure S8). This system, referred to as cage-**1**, consists of four zinc(II) dimers with two distinct metal centers with different coordinated ligands. Each zinc atom is bridged by three carboxylates (Figure 3). Two zinc dimers are further connected through a hydroxide bridge, a coordination mode that is apparently without precedent in single crystal structures of zinc dimers (Table S1). This large cage-like structure can also be considered as consisting of two relatively small cages (Figure 3) that are connected via two bridging ligands **1** (labeled in blue in Figure 3). These bridge-like ligands **1** are bound to two different zinc centers (Figure S10 and Table S1). The distance between the pyridine nitrogen atoms in the opposing bridge-like ligands is 22.341 Å (N−N), while the distance between the two hydroxide bridges is 7.647 Å (O−O, Figure S10).

The solvent, DMF, appears to play a significant role in stabilizing the cage-like assembly produced from $Zn(acac)_2$ and **1**. One function of the DMF molecules is to fill the empty cavities within the structure. The pyrrole and pyridine subunits that make up ligand **1** could potentially compete with the carboxylate functionality for the added zinc cations. No such competition is evident in cage-**1**, a finding that may reflect the presence of DMF molecules within the pyridine-dipyrrolate ligand cleft. The DMF may also influence the structure by binding to the ligands outside of the individual cages (cf. Figure 3 and S10). Two of these external DMF molecules form stable hydrogen bonds with the N−H functionality of nearby pyrroles (N−O = 2.905 and 2.990 Å, Figure S11). Based on the metric parameters, it is likely that interaction causes the two pyrrole subunits within a given ligand to point inward with the result that the NCCN dihedral angles between pyrroles and neighboring pyridines are 6.97° and 13.07°, respectively (Figure S11). These values stand in marked contrast to what

DOI: 10.1021/jacs.6b00564
J. Am. Chem. Soc. 2016, 138, 4573−4579

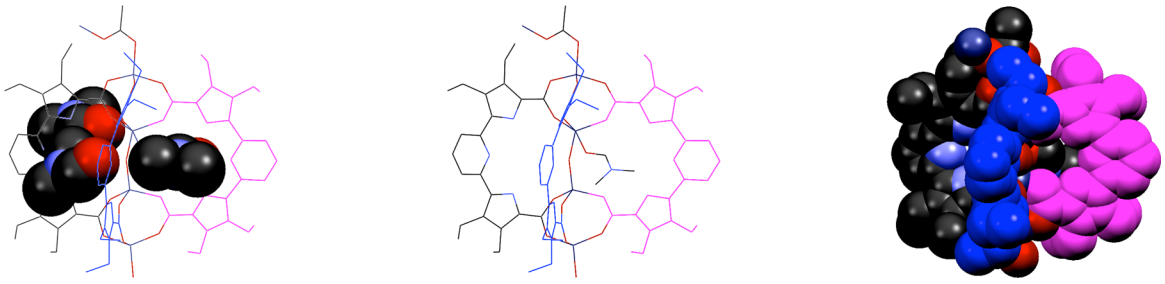

Figure 4. Asymmetric unit of crystal structures of cage-**2** viewed from side in wireframe and space-filling representations. The different subunits of **1** that make up the structure are shown in blue, magenta, and CPK coding, respectively. Solvent molecules are shown in space-filling form in the structure on the left but omitted for clarity in the other views. The hydrogen atoms are omitted for clarity.

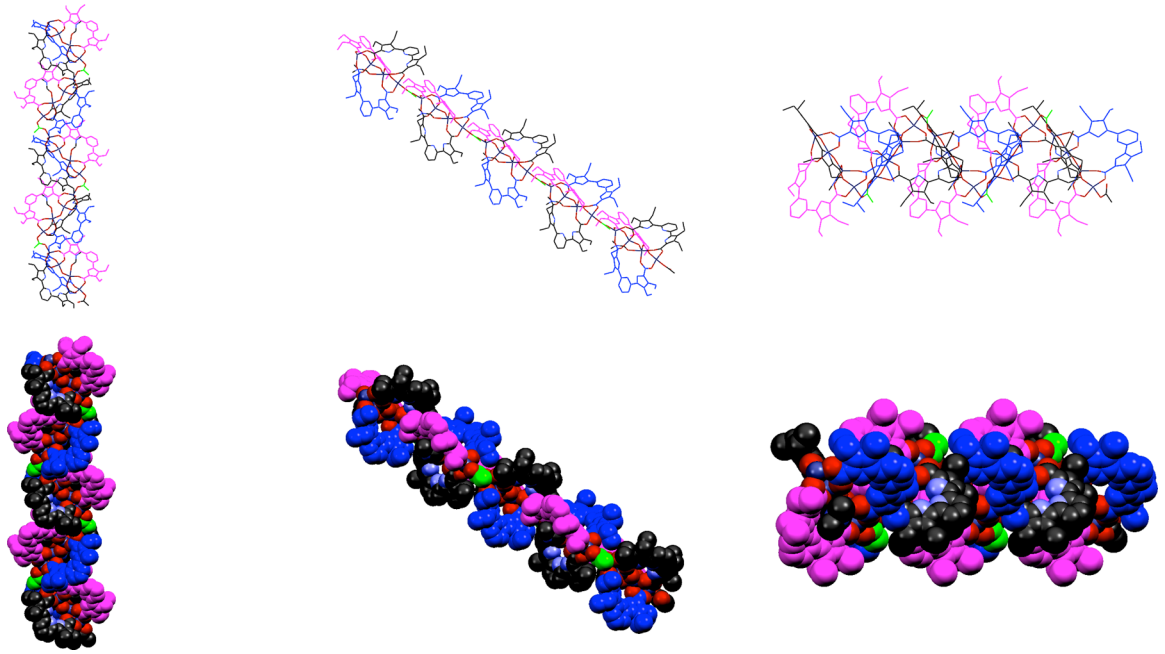

Figure 5. Crystal structures of five units of the infinite polymeric structure referred to as cage-**2** viewed along the *a* axis (left), *b* axis (middle) and *c* axis (right) in wireframe (top) and space-filling (bottom) representations. The subunits of **1** in the structure are labeled in blue, magenta, and CPK coding, respectively. The acetate anion is labeled in green. The hydrogen atoms and solvent molecules are omitted for clarity.

is are quite different from those observed in the single crystals of the metal-free ligand **1** (corresponding angles = 4.73° and 160.7°, respectively; cf. Figure 1). The formyl groups from two other DMF molecules bound outside the cage form hydrogen bonds with the pyrrole N−H on adjacent pyrroles (N−O distances = 3.063 and 3.027 Å) while also interacting via hydrogen bonds with the N−H groups of dimethylammonium ions bound inside the cage (O−N separation = 2.875 Å). These dimethylammonium ions are thought to have their origin in breakdown of the DMF solvent under conditions of crystallization. They are involved in addition hydrogen bonding interactions with the C═O from a nearby carboxylate groups (O−N = 2.673 and 2.737 Å). The center of the cage also contains two DMF molecules as shown in Figure 3. The formyl groups on these DMF molecules interact via hydrogen bonds not only with the N−H (N−O distance = 2.957 Å) subunit of a single neighboring pyrrole. Because only one pyrrole interacts with DMF in this latter instance, the pyrrole and pyridine subgroups are twisted slightly (NCCN dihedral angles = 33.68° and 16.08°), as compared to its opposing ligand (NCCN dihedral angles = 17.36° and 11.06°). The bound DMF molecules also interact with the hydroxide bridge (O−O separation = 2.923 Å). Presumably, the sum total of these interactions, combined with the zinc(II) complexation by the carboxylate functionality present in **1**, gives rise to the observed cage-**1** structure.

Construction of Polymeric Cage-2 Using $Zn(OAc)_2$. Very different behavior is seen when $Zn(OAc)_2$ is used as the Zn(II) cation source under conditions identical to those used above (Scheme 1). Again, clear UV−vis and fluorescent spectral changes are observed in the sample solution (Figure S6 and S7). However, they differ from what is seen in the case of the $Zn(acac)_2$. A significant red-shift is found for the absorption peak at 312 nm when **1** is treated with $Zn(OAc)_2$, a finding that is consistent with a linear aggregate being formed under these solution phase conditions (Figure 2 and S6). A fluorescent emission spectral Job's plot analysis (Figure S8) was not fully consistent with formation of a complex with net 1:1 ligand cation stoichiometry. Rather, an excess of zinc(II) appears involved in the solution phase equilibrium chemistry.

Further insight into the binding interactions were obtained from solid state structural analyses. Colorless single crystals of the solid material generated upon treatment of **1** with $Zn(OAc)_2$ were obtained by using the same vapor diffusion

DOI: 10.1021/jacs.6b00564
J. Am. Chem. Soc. 2016, 138, 4573−4579

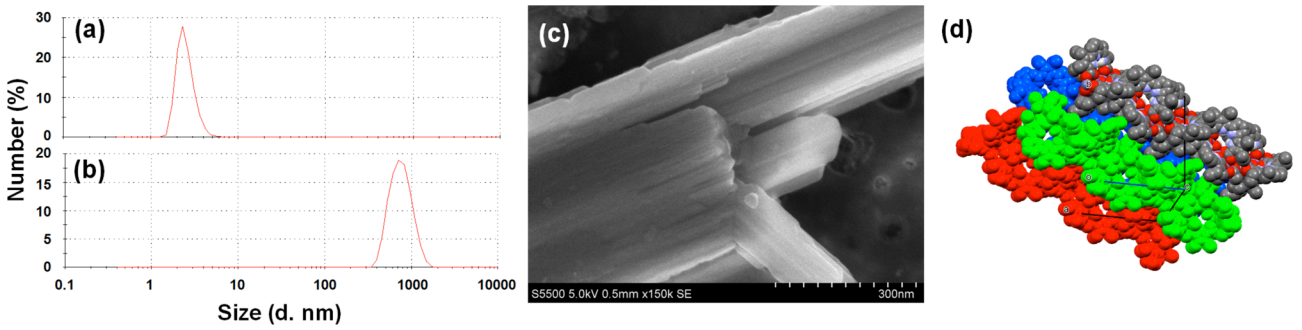

Figure 6. DLS size distributions of compound **1** (1 mM) in the presence of (a) $Zn(acac)_2$ or (b) $Zn(OAc)_2$ at room temperature. (c) SEM image of rod-like assemblies obtained from solution samples prepared from compound **1** and $Zn(OAc)_2$ (1 mM, scale bar = 300 nm). All samples were prepared in 1/5 (v/v) mixture of DMF and MeOH. (d) View of the single crystal X-ray diffraction structure of cage-**2** showing the extended packing present in the solid state. Five units of polymeric cage-**2** are shown in spacefilling form and are labeled in red, green, blue, with standard CPK coding, respectively. Hydrogen atoms and DMF solvent molecules are omitted for clarity.

method as that used to obtain crystals of cage-**1**. X-ray crystallographic analysis provided evidence that a polymeric ensemble (cage-**2**) is obtained in the solid state (cf. Figure 4 and 5). In this structure, the ratio between ligand **1** and the zinc(II) cations is 3:4. Compared to cage-**1**, a molecule of ligand **1** that served as a double bridge between two subunits in cage-**1**, has been replaced by the acetate counterion. The net result is formation of an infinite abacus-like polymeric structure.

Within cage-**2** the individual cage subunits bear resemblance to those present in cage-**1**. For example, the NCCN dihedral angles between the pyrroles and neighboring pyridines in cage-**2** are characterized by values (7.08−26.54°, Figure S12) that are similar to the corresponding ones in cage-**1**. On the other hand, the zinc dimers present in cage-**2** differ from those in cage-**1**. For example, the acetate counteranion participates in the formation of the individual zinc dimer, and further couples two zinc dimers together. One of the bound solvent molecules, H_2O, forms intermolecular hydrogen bonds with the N−H proton on the pyrrole while another solvent, DMF, interacts with one of the zinc centers. This change in coordination environment about the metal center leads to dramatic changes in the metric parameters as compared to cage-**1** (Table S1).

In effort to elucidate the putative role of solvent molecules and counteranions in stabilizing cage-**2**, a control experiment was also carried out. In this experiment, palladium acetate ($Pd(OAc)_2$) was used in combination with $Zn(acac)_2$. Under these conditions, only cage-**2** was obtained, at least in isolatable form with no evidence of Pd(II) complexation being observed.[25]

On this basis, we conclude that both solvent molecules or the counteranion, or both, act as templates; they stabilize intermolecular hydrogen bonding interactions and serve to fix the geometries of compound **1** within the final cage-containing systems.

DLS and SEM Studies. Dynamic light scattering (DLS) and scanning electron microscopy (SEM) studies were employed to obtain additional insights into the solution phase features of the present metal-directed assemblies. As a control, the DMF solution containing pure compound **1** was also subject to analysis by DLS. As shown in Figure S13, DLS indicates that assemblies with an average diameter of around 295 nm are observed in DMF solutions of **1**. These findings match with the conclusions obtained from both single crystal X-ray diffraction (Figure 1) and VT ^{1}H NMR spectroscopic analyses (Figure S1). In comparison with the relatively small mean diameter of 2.7 nm obtained by DLS using a mixed solution of DMF and MeOH (1/5, v/v) containing **1** and $Zn(acac)_2$, a corresponding sample solution obtained using $Zn(OAc)_2$ gave a mean particle size of 825 nm (Figure 6), as would be expected qualitatively given the larger ensemble seen in the solid state for cage-**2** vs cage-**1**. In both cases, the size of the metal-directed assemblies differ from those observed for DMF solutions of pure **1** (Figure S13). Furthermore, the supramolecular ensembles produced from **1**, as well as both cage-**1** and cage-**2** are stable in solution for at least 24 h as inferred from time-dependent DLS analyses (Figure S13).

Rod-like assemblies are also observed in the SEM images of samples made up from solutions (DMF/MeOH in 1/5, v/v) containing compound **1** and $Zn(OAc)_2$. The ensembles observed by SEM using these samples are characterized by an average length of ca. 0.9 μm and an average width of around 30 nm (cf. Figure 6c). Smaller fiber-like features are observed at the ends of the rod-like assemblies. It is likely that the individual abacus-like polymers of cage-**2** further aggregate to produce the large rod-like assemblies in DMF/MeOH (1/5, v/v) observed by SEM and seen in the solid state packing diagram obtained via solid state crystallographic analysis (Figure 6d). No evidence of large structures could be seen by SEM in the case of cage-**1**. This highlights further the ability of ligand **1** to distinguish between two ostensibly similar zinc(II) cation salts, namely $Zn(acac)_2$ and $Zn(OAc)_2$, not just in the solid state, but also under solution phase conditions.

■ CONCLUSIONS

In conclusion, a novel pyridine-pyrrolate ligand, compound **1** has been designed and synthesized. This ligand forms supramolecular polymers through hydrogen bonds in the solid state. In addition, compound **1** is stabilized as a dimer upon the addition of TBAOAc. It acts as an effective ligand for zinc(II) cations and has been found to form two different cage structures when the complexation chemistry is carried out using $Zn(acac)_2$ and $Zn(OAc)_2$ as the cation sources. One of these cage structures, cage-**1**, contains unique zinc dimers and an overall structure stabilized by hydroxide anion bridges and hydrogen bonding interactions involving the bound solvent molecule, DMF. The other cage structure, cage-**2**, consists of an infinite polymeric array wherein the acetate counteranion acts as a bridge to connect two neighboring cage subunits together. In the case of cage-**2**, the formation of rod-like assemblies in solutions was confirmed by DLS and SEM, whereas optical

DOI: 10.1021/jacs.6b00564
J. Am. Chem. Soc. 2016, 138, 4573−4579

analyses served to reveal differences in both the absorption and emission spectra in the case of cage-**1** and cage-**2**. The present system thus allows two different zinc(II) forms to be distinguished readily. It also serves to highlight how differing structures may be stabilized using an appropriately designed ligand system, in this case the angled precursor ligand **1**, under what appear to be rather similar reaction conditions. As such, the findings reported here may set the stage for the creation of yet-more elaborate self-assembled systems while concurrently furthering our understanding the determinants that underlie both metal-based and metal-free self-assembly.

■ ASSOCIATED CONTENT

Supporting Information

The Supporting Information is available free of charge on the ACS Publications website at DOI: 10.1021/jacs.6b00564.

Synthetic procedure and characterization data of compounds **1**−**5**, detailed crystallographic experimental and data for compound **1**, zinc dimers, cage-**1** as well as polymeric cage-**2**, ^{1}H, ^{13}C and VT NMR, DLS, UV−vis, and fluorescent spectral data (PDF)

Crystal data for the dimer of **1** (CIF)

Crystal data for cage-**2** (CIF)

Crystal data for supramolecular polymer of **1** (CIF)

Crystal data for cage-**1** (CIF)

■ AUTHOR INFORMATION

Corresponding Author

*sessler@cm.utexas.edu

Notes

The authors declare no competing financial interest.

■ ACKNOWLEDGMENTS

The work was financially supported by the National Institutes of Health (Grant CA 068682) and the Robert A. Welch Foundation (Grant F-1018).

■ REFERENCES

(1) (a) Kim, D. S.; Sessler, J. L. *Chem. Soc. Rev.* **2015**, *44*, 532. (b) Yu, G.; Jie, K.; Huang, F. *Chem. Rev.* **2015**, *115*, 7240. (c) Peng, H. Q.; Niu, L. Y.; Chen, Y. Z.; Wu, L. Z.; Tung, C. H.; Yang, Q. Z. *Chem. Rev.* **2015**, *115*, 7502. (d) Sun, X.; James, T. D. *Chem. Rev.* **2015**, *115*, 8001. (e) Li, H.; Zhang, H.; Lammer, A. D.; Wang, M.; Li, X.; Lynch, V. M.; Sessler, J. L. *Nat. Chem.* **2015**, *7*, 1003.

(2) Leenders, S. H.; Gramage-Doria, R.; de Bruin, B.; Reek, J. N. *Chem. Soc. Rev.* **2015**, *44*, 433.

(3) (a) Zhang, H.; Zou, R.; Zhao, Y. *Coord. Chem. Rev.* **2015**, *292*, 74. (b) Cook, T. R.; Stang, P. J. *Chem. Rev.* **2015**, *115*, 7001.

(4) (a) Zhang, H.; Grüner, G.; Zhao, Y. *J. Mater. Chem. B* **2013**, *1*, 2542. (b) Xue, M.; Yang, Y.; Chi, X.; Yan, X.; Huang, F. *Chem. Rev.* **2015**, *115*, 7398. (c) Zhou, X.; Lee, S.; Xu, Z.; Yoon, J. *Chem. Rev.* **2015**, *115*, 7944.

(5) (a) Fujita, M.; Tominaga, M.; Hori, A.; Therrien, B. *Acc. Chem. Res.* **2005**, *38*, 369. (b) Inokuma, Y.; Kawano, M.; Fujita, M. *Nat. Chem.* **2011**, *3*, 349. (c) Inokuma, Y.; Yoshioka, S.; Ariyoshi, J.; Arai, T.; Hitora, Y.; Takada, K.; Matsunaga, S.; Rissanen, K.; Fujita, M. *Nature* **2013**, *495*, 461.

(6) McConnell, A. J.; Wood, C. S.; Neelakandan, P. P.; Nitschke, J. R. *Chem. Rev.* **2015**, *115*, 7729.

(7) Yam, V. W.; Au, V. K.; Leung, S. Y. *Chem. Rev.* **2015**, *115*, 7589.

(8) (a) Sanmartín, J.; Bermejo, M. R.; García-Deibe, A. M.; Rivas, I. M.; Fernández, A. R. *J. Chem. Soc., Dalton Trans.* **2000**, 4174. (b) Atilgan, A.; Tanriverdi Ecik, E.; Guliyev, R.; Uyar, T. B.; Erbas-Cakmak, S.; Akkaya, E. U. *Angew. Chem., Int. Ed.* **2014**, *53*, 10678.

(9) (a) Frischmann, P. D.; Kunz, V.; Wurthner, F. *Angew. Chem., Int. Ed.* **2015**, *54*, 7285. (b) Lee, H.; Noh, T. H.; Jung, O. S. *Dalton Trans.* **2014**, *43*, 3842.

(10) Lu, X.; Li, X.; Cao, Y.; Schultz, A.; Wang, J. L.; Moorefield, C. N.; Wesdemiotis, C.; Cheng, S. Z.; Newkome, G. R. *Angew. Chem., Int. Ed.* **2013**, *52*, 7728.

(11) Dong, J.; Zhou, Y.; Zhang, F.; Cui, Y. *Chem. - Eur. J.* **2014**, *20*, 6455.

(12) (a) Liu, H.-K.; Sun, W.-Y.; Ma, D.-J.; Tang, W.-X.; Yu, K.-B. *Chem. Commun.* **2000**, 591. (b) Oppel, I. M.; Focker, K. *Angew. Chem., Int. Ed.* **2008**, *47*, 402. (c) Sorensen, A.; Castilla, A. M.; Ronson, T. K.; Pittelkow, M.; Nitschke, J. R. *Angew. Chem., Int. Ed.* **2013**, *52*, 11273. (d) Gidron, O.; Ebert, M. O.; Trapp, N.; Diederich, F. *Angew. Chem., Int. Ed.* **2014**, *53*, 13614.

(13) Balloch, L.; Garden, J. A.; Kennedy, A. R.; Mulvey, R. E.; Rantanen, T.; Robertson, S. D.; Snieckus, V. *Angew. Chem., Int. Ed.* **2012**, *51*, 6934.

(14) Aoki, S.; Shiro, M.; Kimura, E. *Chem. - Eur. J.* **2002**, *8*, 929.

(15) (a) Baldini, L.; Ballester, P.; Casnati, A.; Gomila, R. M.; Hunter, C. A.; Sansone, F.; Ungaro, R. *J. Am. Chem. Soc.* **2003**, *125*, 14181. (b) Oliva, A. I.; Ventura, B.; Wurthner, F.; Camara-Campos, A.; Hunter, C. A.; Ballester, P.; Flamigni, L. *Dalton Trans.* **2009**, 4023. (c) Taesch, J.; Heitz, V.; Topic, F.; Rissanen, K. *Chem. Commun.* **2012**, *48*, 5118. (d) Nakamura, T.; Ube, H.; Miyake, R.; Shionoya, M. *J. Am. Chem. Soc.* **2013**, *135*, 18790. (e) Nakamura, T.; Ube, H.; Shiro, M.; Shionoya, M. *Angew. Chem., Int. Ed.* **2013**, *52*, 720. (f) Zhu, B.; Chen, H.; Lin, W.; Ye, Y.; Wu, J.; Li, S. *J. Am. Chem. Soc.* **2014**, *136*, 15126.

(16) Lee, E.; Ju, H.; Kang, Y.; Lee, S. S.; Park, K. M. *Chem. - Eur. J.* **2015**, *21*, 6052.

(17) Xiao, X.; Chen, K.; Xue, S.-F.; Zhu, Q.-J.; Tao, Z.; Wei, G. *J. Mol. Struct.* **2010**, *969*, 216.

(18) (a) Power, N. P.; Dalgarno, S. J.; Atwood, J. L. *Angew. Chem., Int. Ed.* **2007**, *46*, 8601. (b) Fowler, D. A.; Rathnayake, A. S.; Kennedy, S.; Kumari, H.; Beavers, C. M.; Teat, S. J.; Atwood, J. L. *J. Am. Chem. Soc.* **2013**, *135*, 12184. (c) Kumari, H.; Deakyne, C. A.; Atwood, J. L. *Acc. Chem. Res.* **2014**, *47*, 3080.

(19) Ni, T. W.; Tezcan, F. A. *Angew. Chem., Int. Ed.* **2010**, *49*, 7014.

(20) (a) O'Keeffe, M.; Yaghi, O. M. *Chem. Rev.* **2012**, *112*, 675. (b) Jiang, J.; Yaghi, O. M. *Chem. Rev.* **2015**, *115*, 6966.

(21) (a) Pal, A. K.; Hanan, G. S. *Chem. Soc. Rev.* **2014**, *43*, 6184. (b) Sakamoto, R.; Wu, K.-H.; Matsuoka, R.; Maeda, H.; Nishihara, H. *Chem. Soc. Rev.* **2015**, *44*, 7698.

(22) Setsune, J.-i.; Watanabe, K. *J. Am. Chem. Soc.* **2008**, *130*, 2404.

(23) Zhang, Z.; Lim, J. M.; Ishida, M.; Roznyatovskiy, V. V.; Lynch, V. M.; Gong, H. Y.; Yang, X.; Kim, D.; Sessler, J. L. *J. Am. Chem. Soc.* **2012**, *134*, 4076.

(24) (a) Liu, Q.; Thorne, L.; Kozin, I.; Song, D.; Seward, C.; D'Iorio, M.; Tao, Y.; Wang, S. *J. Chem. Soc., Dalton Trans.* **2002**, 3234. (b) Jia, W.-L.; Liu, Q.-D.; Wang, R.; Wang, S. *Organometallics* **2003**, *22*, 4070.

(25) Komine, N.; Buell, R. W.; Chen, C. H.; Hui, A. K.; Pink, M.; Caulton, K. G. *Inorg. Chem.* **2014**, *53*, 1361.

(26) Chinchilla, R.; Nájera, C.; Yus, M. *Chem. Rev.* **2004**, *104*, 2667.

(27) Setsune, J.-i.; Toda, M.; Watanabe, K.; Panda, P. K.; Yoshida, T. *Tetrahedron Lett.* **2006**, *47*, 7541.

(28) Vogel, E.; Koch, P.; Hou, X.-L.; Lex, J.; Lausmann, M.; Kisters, M.; Aukauloo, M. A.; Richard, P.; Guilard, R. *Angew. Chem., Int. Ed. Engl.* **1993**, *32*, 1600.

(29) UV and fluorescence spectroscopic titrations were performed using excess $Zn(acac)_2$ and $Zn(OAc)_2$ (Figure S6 and S7). On the basis of these studies, we believe that at stoichiometric ratios greatly exceeding 1:1 (Zn^{2+} to 1) more complex species are formed than the cages we have characterized to date. Efforts to elucidate the structures of those putative new species are ongoing.

DOI: 10.1021/jacs.6b00564
J. Am. Chem. Soc. 2016, 138, 4573−4579